THE AMERICAN MINERALOGIST, VOL. 52, NOVEMBER-DECEMBER, 1967

CHLORITE POLYTYPISM: IV. REGULAR TWO-LAYER STRUCTURES

JUDITH S. LISTER AND S. W. BAILEY, *Department of Geology, University of Wisconsin, Madison, Wisconsin.*

ABSTRACT

Theoretical 2-layer chlorite polytypes may be classified according to 64 unique [010] projection groups. These groups contain a total of 1134 unique individual 2-layer polytypes, of which 1009 have a monoclinic-shaped unit cell and 125 have an orthorhombic-shaped unit cell. Natural 2-layer specimens are rare; representatives of only three of the [010] projection groups have been found to date. Most of these 2-layer structures belong to two of the projection groups and are composed of only a single structural layer type, either I*a* or II*b*. The third natural group is different in that the structures contain 2-layer packets made up of two different layer types. Several crystals of purple Cr-chlorite from Erzincan, Turkey, which belong to this third group, have been studied in detail.

The apparent space group of one of the 2-layer Erzincan crystals is $C1$ with $a=5.335$, $b=9.240$, $c=28.735$ Å, and $\alpha=\beta=\gamma=90°$. The ideal model on which the structure is based has a *c*-glide plane perpendicular to the short axis. This symmetry plane is destroyed by an ordered distribution of the Cr atoms within the brucite sheet over positions not related by a *c*-glide. The 2-layer repeat is due to a regular alternation of octahedral cations between I and II sites in both the talc and brucite sheets of the two layers. The talc network is distorted by 6° planar rotations of the tetrahedra. The crystal is twinned and is made up of six roughly triangular sectors. The six sectors comprise two interpenetrating sets of three members each, believed to be related by a rotation of 180° about the [010] axis. Composition planes are (100), (130), and (1$\bar{3}$0). All crystals containing 2-layer packets are twinned and are elongate along *Z*. The twinning has prevented complete refinement of the structure.

INTRODUCTION

In part I of this study of chlorite polytypism Bailey and Brown (1962) showed that four different types of chlorite layers, designated I*a*, I*b*, II*a*, and II*b*, are theoretically possible. Layers of the same type can be superimposed to form twelve unique 1-layer polytypes having a regular stacking sequence and six structures having a semirandom stacking sequence. Of the four basic layer types, all except the II*a* type have been recognized in natural specimens.

In addition to 1-layer and semirandom structures, several regular multiple-layer polytypes are known to exist. Brindley *et al.* (1950) recognized some multiple-layer chlorite polytypes, including a 2-layer variety having a monoclinic-shaped cell. All of the layers in these multiple-layer structures are of the same strucutral type, II*b*. Two different 2-layer monoclinic polytypes of cookeite, a Li-Al dioctahedral chlorite, also are made up of a single layer type, in this case the I*a* layer (Lister, 1966). Drits (1966) has reported a 2-layer Al-Mg dioctahedral chlorite containing II*b* type layers. Vermiculite, which is very similar to chlorite in structure, has been described by Mathieson and Walker (1954) and

by Shirozu and Bailey (1966) as occurring in at least two different 2-layer structures involving I*a* type layers. Oughton, as reported by Brindley (1961), found a 2-layer kämmererite crystal having an orthorhombic-shaped unit cell, but no details from which the nature of the layer type could be determined were reported.[1] Frondel (1955) described a 2-layer Mn-chlorite, gonyerite, which has an orthorhombic-shaped cell, but no conclusion has been made as to its layer type.

The present study of regular 2-layer structures was prompted by the discovery of a natural 2-layer Cr-chlorite more complex than others reported to date. This polytype, instead of being made up of only one type of layer, is a 2-layer packet composed of a combination of two different layer types. The *h*0*l* intensity data for this combination of layer types is different from those for which only one layer type is present. To facilitate selection of a trial model a systematic study was made of all theoretically possible 2-layer structures. The results of the theoretical study and of the determination of the 2-layer Cr-chlorite structure are presented in this paper.

Derivation of 2-Layer Polytypes

In a study of theoretically possible 2-layer chlorite polytypes many more variables need to be considered than in the case of 1-layer structures. Bailey and Brown (1962), in their study of 1-layer polytypes, showed that there are four possible ways of positioning the brucite sheet on the initial talc sheet and six positions that may be assumed by the repeating talc sheet. They found that they needed to consider only four of the six possible positions for the repeating talc sheet since certain structures are equivalent to others after being rotated 180° about the *y* axis or because of an enantiomorphic relationship. In 2-layer polytypes these equivalences of individual 1-layer structures must be disregarded because each l-layer unit is no longer unique but is part of a 2-layer structure. Thus all six possible positions of the repeating talc sheet must be considered. To complicate further the derivation of the 2-layer structures, the orientation of the talc sheet need not be identical in each successive layer as is true for regular 1-layer structures, and shifts within the talc sheet itself also need to be considered.

If the cation sites in the octahedral part of the talc sheet are selected so that in projection the triangle of cations surrounding the OH points to the south, site I in this discussion, the upper tetrahedral sheet can be

[1] Rotation photographs of this chlorite from Lake Iktul, Ural Mountains, were kindly made available to us by Oughton as this paper went to press. The structural type is similar to that of the 2-layer Erzincan chlorite described in this paper, except that all $k \neq 3n$ reflections are continuous streaks as in Fig. 5*b*.

displaced relative to the lower tetrahedral sheet only along the negative x_1, x_2, or x_3 axes if close packing of the octahedral anions is to be preserved. However if the alternate site for the octahedral cations is chosen, site II in this paper, so that in projection the triangle of cations around the OH points north, the upper tetrahedral sheet may only be shifted along the positive x_1, x_2, or x_3 axes (Fig. 1). These last three arrangements correspond to the L, N, amd M structures, respectively, of Brindley *et al.* (1950). In referring to the talc sheets in the following discussion, those built up with site I occupied will be designated $\bar{x}_1$, $\bar{x}_2$, or $\bar{x}_3$, depending on whether the shift has been along a negative x_1, x_2, or x_3 axis respectively.

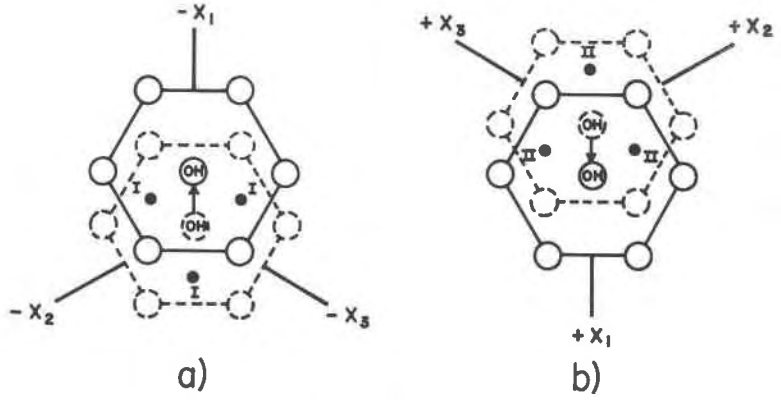

FIG. 1. Diagram of the octahedral portion of the talc sheet. The lower O-OH anion plane is drawn with dashed lines. Occupation of cation site I requires a shift of the upper anion plane along the $-x$ axis and occupation of cation site II requires a shift of the upper anion plane along the $+x$ axis to maintain close packing of octahedral anions.

Those built up with site II occupied will be called x_1, x_2, or x_3, corresponding to a shift along the positive x_1, x_2, or x_3 axis respectively. In this manner the terminology will have meaning in reference to a fixed crystallographic orientation. It should be noted that the crystallographic axes of the resultant structure may not coincide with the fixed axes used in the theoretical polytype derivation.

To describe completely a 2-layer chlorite polytype six terms need to be used. Each chlorite layer is described separately according to the terminology of Bailey and Brown (1962) and one additional term is added to describe the variables within the talc sheet of each layer. For an example of how the description of a polytype is set up we consider the structure of $\bar{x}_1$-I*a*-5 : x_2-II*b*-3. The first term is the symbol representing the shift within the initial talc sheet, as shown in Fig. 1*a*. This term automatically

indicates the choice of octahedral cation site. Possibilities are $\bar{x}_1$, $\bar{x}_2$, $\bar{x}_3$, or x_1, x_2, x_3, cation sites I and II respectively. The symbol describing the talc sheet variable is followed by the symbol for the type of brucite sheet. Possibilities are I*a*, I*b*, II*a*, or II*b*. Finally, the position of the talc sheet of the second layer relative to the brucite sheet of the first layer is represented by a number, 1, 2, 3, 4, 5, or 6. To avoid any possible confusion in applying the definitions of these six positions to 2-layer structures, it should be pointed out that the six positions may not always be distributed about a N-S mirror plane in the talc sheet below, as is illustrated for 1-layer chlorites in Part I, Fig. 3 (Bailey and Brown, 1962), due to

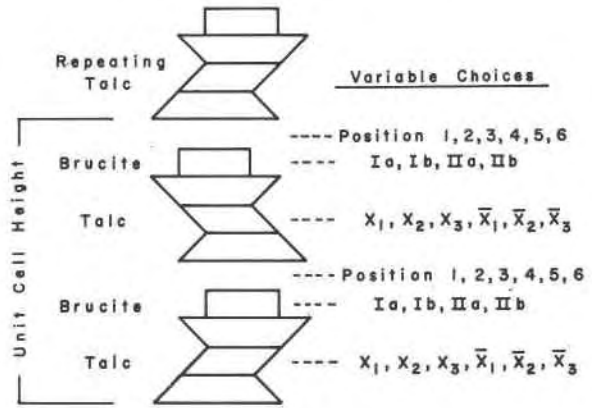

FIG. 2. Diagram illustrating the variables in the stacking sequence of a 2-layer chlorite.

the possibility of shifts along the x_2 and x_3 axes. The numbering system remains as given in Fig. 3 of Part I but the arrow should be relabeled as the $-x_1$ direction of the initial talc sheet. The central OH of the figure must lie on the mirror plane of the talc sheet below, but that plane may be oriented so that it intersects either sites 1–2, 4–5, or 6-3. The second layer is described in a similar manner, using the same fixed axes as for the first layer (Fig. 2). One consequence of using the fixed axes of the first layer to describe the second layer as well is that layer symbols may be derived that do not correspond to the unique 1-layer polytypes selected in Part I. For example, a symbol $\bar{x}_2$-I*a*-2 may be derived for a layer that would be designated $\bar{x}_1$-I*a*-6 (or simply I*a*-6) if it occurred as a 1-layer structure. The layer type symbol may change also, as from I*a* to II*a*.

Summarizing the variables for a single layer, there are six ways to build up the talc sheet, four different arrangements for the brucite sheet,

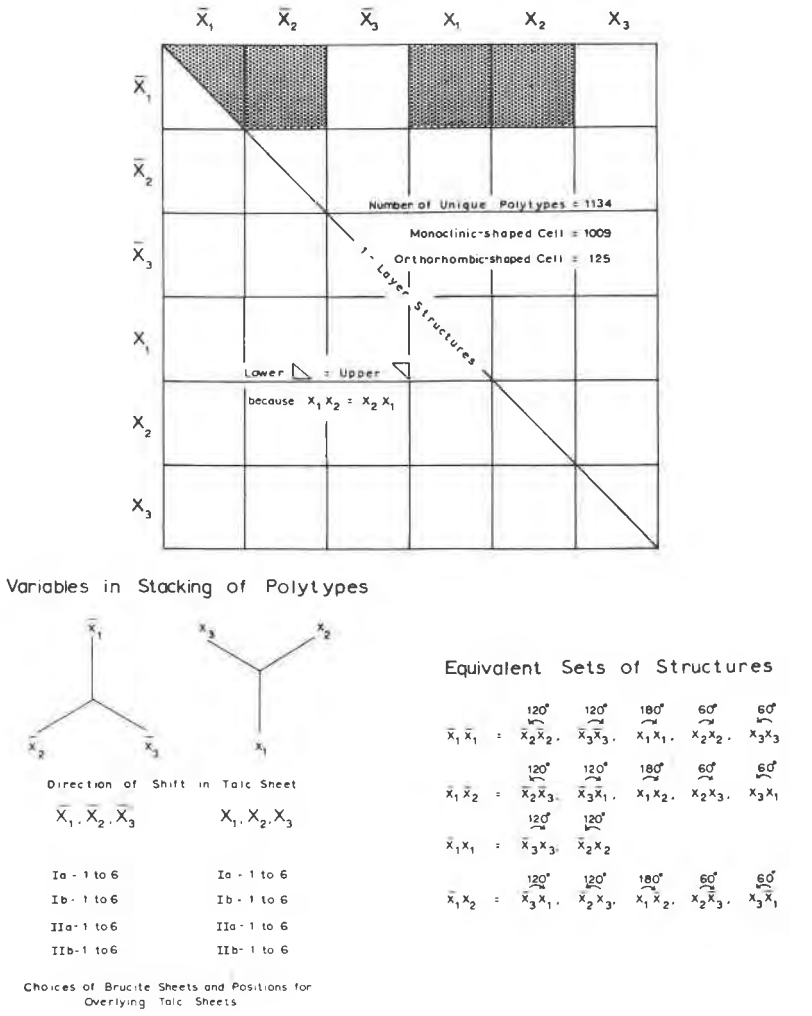

FIG. 3. Diagram showing the four sets (shaded) containing the unique 2-layer polytypes. Each square represents the polytypes that may be built up with a specific combination of two talc sheets and all possible combinations of brucite sheets. Groups of structures along the diagonal are 1-layer in [010] projection and certain individual structures in these groups are 1-layer in 3-dimensions. See discussion of sets $\bar{x}_1\bar{x}_1$ and $\bar{x}_1\bar{x}_2$ in text. An individual square is shown in more detail in Fig. 4.

and six different positions for the next talc sheet. This means that for a fixed orientation there are 144 different 1-layer types that may be combined with one another to form the 2-layer polytypes. The number of different 2-layer polytypes possible, still considering the fixed orientation,

can be expressed by the following equation, where n = number of 1-layer forms.

$$\text{Number of theoretical 2-layer polytypes} = (n^2 - n)/2 = 10{,}296$$

Fortunately, it was discovered with the aid of stacking models that many of these structures are equivalent to one another after being rotated 60°, 120°, or 180° around an axis perpendicular to (001). Figure 3 outlines this information. These equivalences reduce the number of polytypes to 2004, of which 225 have orthorhombic-shaped unit cells. Equivalences between structures after rotations of 180° around y can also be established. Considering all these equivalences, the probable number of unique 2-layer polytypes is 1134, 125 having orthorhombic-shaped cells and 1009 having monoclinic-shaped cells. All of the unique polytypes can be oriented so that the shift within the initial talc sheet is along negative x_1, as in Figure 1*a*. The second layer shift then can be directed along either the x_1 or x_2 axes, positive or negative. These unique polytypes are contained within the shaded sets of Figure 3.

Equivalences of structures after 180° rotation around Y are more easily recognized if the individual polytypes are grouped according to [010] projection, of which there are only 64 unique types. Figure 4 shows in more detail the four sets of Figure 3 that contain unique polytypes. Each of the small squares in Figure 4 represents a group of nine individual polytypes, all having the same [010] projection. The symbols $\bar{x}_1$,

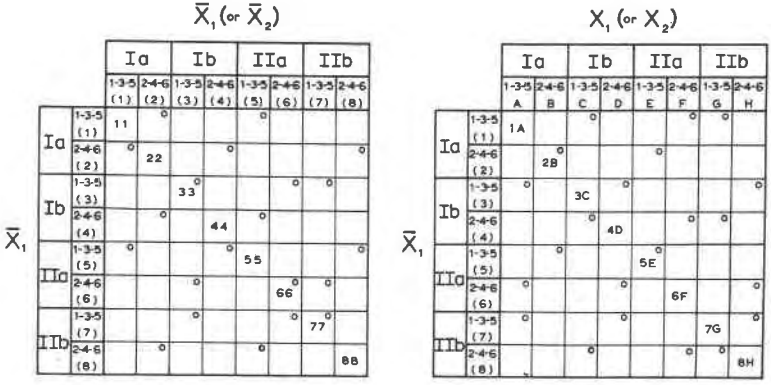

FIG. 4. Diagram showing the number of different [010] projections for 2-layer chlorite structures. Each small square represents nine individual polytypes having the same [010] projection but different 3-dimensional structures. Some projections are equivalent after rotation of the structures 180° around the y axis. Letters and numbers in parentheses are used to distinguish the different 1-layer projections that are combined to yield the 2-layer structures. Groups containing some individual structures with an orthorhombic-shaped cell are marked with an 0.

$\bar{x}_2$, x_1, and x_2 identify the sets defined in Fig. 3 on the basis of different combinations of talc sheets. A choice of either $\bar{x}_1$ or $\bar{x}_2$ (or x_1 or x_2) for the second layer does not change the [010] projection. The numbers 1-3-5 and 2-4-6 represent the choices of position of the repeating talc sheet.

For ease of listing the equivalent two-layer projections, each single-layer projection in Fig. 4 has been identified by a letter or by a number in parentheses. Members of row 1 are equivalent to members of row D (or 4), row 2 = B (or 2), row 3 = C (or 3), row 4 = A (or 1), row 5 = E (or 5), row 6 = G (or 7), row 7 = F (or 6), and row 8 = H (or 8). From this it follows that the equivalent projections for the $\bar{x}_1x_1$ set of 2-layer structures are as listed below.

1A=4D	2A=4B	3A=4C	4A=4A	5A=4E	6A=4G	7A=4F	8A=4H
1B=2D	2B=2B	3B=2C	4B=2A	5B=2E	6B=2G	7B=2F	8B=2H
1C=3D	2C=3B	3C=3C	4C=3A	5C=3E	6C=3G	7C=3F	8C=3H
1D=1D	2D=1B	3D=1C	4D=1A	5D=1E	6D=1G	7D=1F	8D=1H
1E=5D	2E=5B	3E=5C	4E=5A	5E=5E	6E=5G	7E=5F	8E=5H
1F=7D	2F=7B	3F=7C	4F=7A	5F=7E	6F=7G	7F=7F	8F=7H
1G=6D	2G=6B	3G=6C	4G=6A	5G=6E	6G=6G	7G=6F	8G=6H
1H=8D	2H=8B	3H=8C	4H=8A	5H=8E	6H=8G	7H=8F	8H=8H

Also, 1D = 7F, 2B = 5E, 3C = 8H, and 4A = 6G on the basis of an enantiomorphic relationship after 180° rotation about y. From this list of equivalent projections 32 unique projections may be selected. As a result there is a total of $32 \times 9 = 288$ unique individual 2-layer polytypes for this set, 33 of which have an orthorhombic-shaped cell and 255 a monoclinic-shaped cell. Set $\bar{x}_1x_2$ contains the same projections but an additional 288 different 2-layer polytypes.

For the $\bar{x}_1\bar{x}_1$ and $\bar{x}_1\bar{x}_2$ sets, which contain identical projections, the list of equivalent projections is the same as for the $\bar{x}_1x_1$ and $\bar{x}_1x_2$ sets after taking into account the substitution of numbers for letters for the second layer columns. Thus, projection 11 = 44, 21 = 42, 31 = 43, etc. In addition, projection 21 = 12 and projection 31 = 13 by reversal of layer order, as do all pairs of projections symmetrically related across the diagonal row. Projections 22, 33, 55, and 88 are unique and are not equivalent to any others. Thus for these two sets there are 32 unique projections.

Special mention must be made of the polytypes in the $\bar{x}_1\bar{x}_1$ set. Individual structures such as $\bar{x}_1$-Ia-1: $\bar{x}_1$-Ia-1, $\bar{x}_1$-1a-3: $\bar{x}_1$-Ia-3, etc. that lie exactly on the diagonal line are true 1-layer structures. Also, individual 2-layer structures that are symmetrically related across the diagonal line are identical in 3-dimensions. This is the case only for the $\bar{x}_1\bar{x}_1$ set and not for the $\bar{x}_1\bar{x}_2$ set, although both sets are the same in [010] projection. For the $\bar{x}_1\bar{x}_1$ set, then, there are 252 unique 2-layer polytypes, of which 26 have an orthorhombic-shaped unit cell. In the $\bar{x}_1\bar{x}_2$ set individual struc-

tures related across the diagonal may not necessarily be equivalent in 3-dimensions even though they have the same [010] projection. Thus, for this set there are probably 306 unique 2-layer polytypes, of which 33 have an orthorhombic-shaped cell. It is possible that further equivalences of projections or of individual structures may exist, but the rarity of different natural 2-layer polytypes does not warrant a more exhaustive study at this time.

For both the $\bar{x}_1\bar{x}_1$ and $\bar{x}_1\bar{x}_2$ sets the individual 2-layer structures that occur in the small squares comprising the diagonal row are 1-layer in [010] projection and include all the previously reported natural 2-layer chlorite and vermiculite polytypes, except gonyerite. These polytypes may be described in the terminology of the present paper as follows:

Brindley *et al.* (1950) chlorite "C"	$\bar{x}_1$-II*b*-6:$\bar{x}_2$-II*b*-4
Mathieson and Walker (1954) vermiculite "r"	$\bar{x}_1$-I*a*-6:$\bar{x}_2$-I*a*-6
Mathieson and Walker (1954) vermiculite "q"	$\bar{x}_1$-I*a*-4:$\bar{x}_2$-I*a*-2
Shirozu and Bailey (1966) vermiculite "s"	$\bar{x}_1$-I*a*-4:$\bar{x}_1$-I*a*-6
Lister (1966) cookeite (1)	$\bar{x}_1$-I*a*-6:$\bar{x}_2$-I*a*-6
Lister (1966) cookeite (2)	$\sim\bar{x}_1$-I*a*-4:$\bar{x}_1$-I*a*-6
Drits (1966) dioctahedral chlorite	$\bar{x}_1$-II*b*-4:$\bar{x}_1$II*b*-6

The same terminology can be extended to chlorites with more than two layers. The 3-layer crystal "D" described by Brindley *et al.* (1950) contains only one structural layer type and would have the symbol $\bar{x}_1$-II*b*-6:$\bar{x}_2$-II*b*-4:$\bar{x}_1$-II*b*-4.

Sample Description and Data for a Natural 2-Layer Cr-Chlorite

An orthohexagonal 2-layer polytype of Cr-chlorite (kämmererite) was identified in a sample contributed by Dr. R. A. Bell from the Erzincan province, Turkey. The chlorite occurs as incrustations on the walls of vugs and cracks in a serpentinized basic rock. According to a chemical analysis by Brown and Bailey (1963) the chlorite has the composition $(Si_3Al)\ (Mg_{5.0}Fe_{0.1}^{2+}Cr_{0.7}Al_{0.2})O_{18}H_{7.9}$. In this well-crystallized chlorite sample several different polytypes have been recognized.

Approximately 90 crystals from the Erzincan sample have been examined in this study and in the study by Brown and Bailey (1963). All except seven of the crystals have either regular 1-layer or semirandom structures of the I*a* layer type. The seven different crystals all contain 2-layer packets, as indicated by the periodicity along *h*0*l* row lines, in which the identification of the layer types is not obvious. Six of the seven crystals have a regular stacking sequence along the *z* axis and give discrete $k \neq 3n$ reflections. The other crystal has a disordered stacking sequence as indicated by a continuous streak taking the place of the $k \neq 3n$ reflec-

tions (Fig. 5). Even this disordered crystal shows a 2-layer periodicity in the *h0l* reflections, however, so that the randomness must involve the stacking of 2-layer packets rather than individual layers.

All of the 2-layer crystals are elongate along the *z*-axis, and those having a regular stacking sequence are twinned. The twin units, visible on the (001) face, are six roughly triangular sectors that comprise two interpenetrating sets of three members each. Members of one set alternate

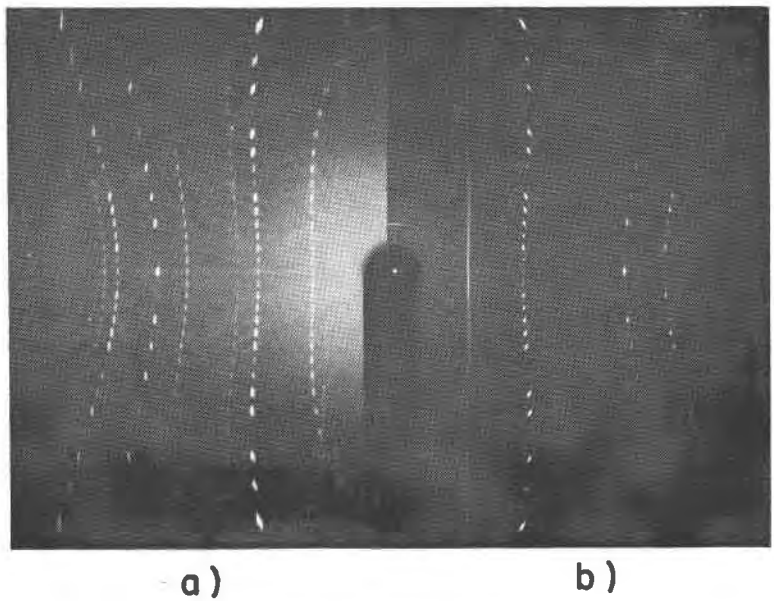

FIG. 5. Rotation photographs taken about Z^* showing: (a) a 2-layer polytype with a regular staking sequence and (b) a 2-layer polytype with a random stacking sequence.

with members of the other set. Fine lines separating the twin sectors can be observed with unpolarized transmitted light. One crystal, which appeared to be representative of the group, was selected for a more detailed optical and X-ray investigation. The refractive indices at the sodium D line (589 mμ) are $\alpha = 1.5970$ and $\beta \cong \gamma = 1.5996$. The slopes of the dispersion curves are different, and the curves cross at a wave length greater than 589 mμ. Optically, one twin set of this crystal is rotated 60° from the other set around an axis perpendicular to the (001) face. Precise extinction angles are difficult to obtain since the crystal is almost uniaxial. There is a zone of strain between the sectors that is pointed out by the greater departure from extinction of the margins of the twin sector compared to that of the center of the sector. The center of certain sectors

shows no noticeable departure from extinction. The optics of this twinned crystal, and those of two others for which both optical data and X-ray precession photographs were obtained, are anomalous. The extinction directions, or apparent extinction directions, are not parallel to the unique crystallographic directions as determined by X-ray methods. There is still some reservation as to whether this anomalous extinction is real or is due to strain at the twin boundaries. For the crystal studied in detail the twin axis is believed to be [010] and the composition plane to be (100) (also (130) and ($1\bar{3}0$)).

The rotation photographs of a crystal having a regular stacking sequence and one having a random stacking sequence (Fig. 5) prove the existence of two-layer packets in both. The observation of 2-layer periodicity in the $h0l$ reflections, rather than in the $0kl$ reflections, requires that the layers in the packet be of different structural types, *i.e.* the octahedral cations must alternate between sites I and II in the talc or brucite sheets, or both of adjacent layers. The different nature of this chlorite is illustrated further by the observation that a small portion of a crystal crushed for a powder photograph gives a pattern different from that of any of the previously recorded theoretical or observed chlorite layer types. Table 1 lists the observed and calculated d values for this powder pattern.

From precession photographs it was determined that the shape of the unit cell is orthorhombic, $\beta = 90°$. The refined cell parameters, $a = 5.335$, $b = 9.240$, and $c = 28.735$ Å, were measured by the θ method of Weisz *et al.* (1948). The unit cell is centered on the (001) face; the reflections present follow the rule $h+k=2n$. Precession photographs show a pseudo c-glide perpendicular to x, as evidenced by $0kl$, $l \neq 2n$ reflections being weak. The $06l$, $l \neq 2n$ reflections are present although much weaker than the other weak $0kl$, $l \neq 2n$ types. The apparent space group of the twin crystal is $C1$. Because of the orthorhombic shape of the unit cell, twin reflections exactly superimpose on the normal reflections.

Several attempts were made to cut out an individual twin sector. Although both the small size of the sectors and imperfections caused by the cutting made it impossible to collect accurate intensity data by the Weissenberg method, some useful precession photographs of an untwinned sector were obtained. These precession photographs confirm that the structure has an orthorhombic-shaped 2-layer cell. In fact, zero level photographs of the twinned crystal and of the cut sectors are identical. This is as one would expect if the untwinned crystal has one or more symmetry planes parallel to z and if the symmetry elements of two different twin sectors are superimposed by the twinning. As observed also for the twinned crystal, the $0kl$, $l \neq 2n$ reflections recorded from the un-

TABLE 1

OBSERVED AND CALCULATED POWDER DATA FOR THE 2-LAYER CR-CHLORITE

hkl	*d* calc (Å)	*d* observed (Å)	I_0
002	14.36	14.46	9
004	7.183	7.206	10
006	4.789	4.809	8
110, 020, 111, 021	4.590	4.619	8
112, 022	4.398	4.412	2
113, 023	4.161	4.175	3
114, 024	3.885	3.899	2
115, 025, 008	3.600	3.600	9
116, 026	3.325	3.334	1
117, 027	3.068	3.076	½
0.0.10, 118, 028	2.873	2.878	4
200, 130, 201, 131	2.661	2.664	3
119, 029, 202, 132	2.626	2.626	8
203, 133	2.569	2.575	4
204, 134	2.500	2.504	8
205, 135, 0.0.12	2.429	2.424	10
206, 136	2.330	2.340	7
223, 043, 207, 137	2.245	2.249	1
225, 045	2.143	2.143	1
0.0.14, 209, 139	2.050	2.050	6
2.0.10, 1.3.10	1.955	1.958	5
2.0.12, 1.3.12	1.781	1.786	4
310, 240, 150	1.746	1.749	1½
312, 242, 152	1.733	1.738	1½
2.0.13, 1.3.13	1.702	1.704	3
2.0.14, 1.3.14	1.626	1.629	4½
2.0.15, 1.3.15	1.556	1.558	3
330, 060	1.540	1.541	9
1.1.18, 0.2.18, 334, 064	1.507	1.507	4½
2.2.15, 0.4.15, 336, 066	1.470	1.468	2
0.0.20	1.436	1.437	1
2.0.17, 1.3.17	1.427	1.429	1
068, 338	1.415	1.416	2

twinned sector are weak and the 06*l*, $l \neq 2n$ reflections are present but very weak.

STRUCTURE DETERMINATION

Intensity data were collected from the twinned crystal for comparison with intensities of twinned trial models in the hope that the true structure and the twin relationship could be deduced. The crystal used had

approximately the shape of a hexagon elongate along the z axis. The length of the crystal was 0.74 mm and its diameter ranged from 0.24 mm at the base to 0.13 mm at the tip. Only a small equidimensional portion cut from the tip was used for most of the structure determination. The volume of the twin segments could be determined more accurately for this segment. A total of 576 reflections was collected by the Weissenberg multiple film pack technique from the $0kl$, $h0l$, $hk0$, and $hk8$ levels, and a standard multiple film pack scale was made for visually estimating the intensities. CuKα radiation was used rather than MoKα because the small spacings of the reciprocal lattice along Z* did not permit the reflections to be separated distinctly with MoKα radiation. A spherical absorption correction, Lorentz-polarization correction, and an $\alpha_1-\alpha_2$ separation correction were applied to the data.

The ideal structural models pertinent to this study are those that have an orthorhombic-shaped cell. To facilitate selection of the "orthorhombic" polytypes, each of the individual single layers was described in terms of a vector whose magnitude and direction was established by joining the lower OH of one talc sheet with the corresponding OH of the next talc sheet above. Combination of layers having equal and opposite vectors yields the structures that have orthorhombic-shaped cells. These vector combinations are 0:0, $+1/3\ b_3:-1/3\ b_3$, $+1/3\ a_1:-1/3\ a_1$, $+1/3\ a_2:-1/3\ a_2$, and $+1/3\ a_3:-1/3\ a_3$. The 21 different [010] projections represented by these "orthorhombic" structures were tested against the observed data by comparing F_0 and F_c. From these tests the projection group 1F (Fig. 4) gave considerably better agreement ($R=16\%$ for 77 reflections) than any other group ($R=25$ to 70%), and was selected as the correct projection. Table 2 includes the ideal coordinates for the [010] projection of this group. There are six unique "orthorhombic" polytypes that have this [010] projection, four with the space group $C1$ and two with the space groups Cc and $Ccm2_1$. Although the apparent space group of the crystal is $C1$, the observed pseudo c-glide requires that the trial model have basically a c-glide character. Of these six polytypes only the Cc and $Ccm2_1$ ideal models, polytype designations $\bar{x}_1$-Ia-3:x_2-IIa-6 and $\bar{x}_1$-Ia-1:x_1-IIa-2 respectively, have any symmetry and are possible choices for the correct structure.

Further discrimination between the Cc and $Ccm2_1$ structures requires that the type of twinning be determined. Twinned models developed by the twin operations of 180° rotation about an axis along one of the directions [100], [110], [1$\bar{1}$0], [310], or [3$\bar{1}$0] (Sadanaga and Takéuchi, 1961), by reflection across (100), and by 180° rotation around [010] were tested for both of these structures by comparison of calculated twin intensities with the observed values. To aid in making the choice, an additional 1081 ob-

TABLE 2

ATOMIC COORDINATES OF IDEAL AND REFINED STRUCTURE

Atom		Ideal[a]			Refined		
		x	y	z	x	y	z
Mg	1	0.000	0.000	0.000	0.000	0.000	0.000
	2	.000	.333	.000	.007	.329	.002 = (Cr_3)
	3	.000	.667	.000	.987	.660	.996
	4	.167	.167	.250	.164	.170	.250
	5	.167	.500	.250	.180	.502	.250
	6	.167	.833	.250	.176	.832	.250
	7	.000	.000	.500	.021	.992	.498
	8	.000	.333	.500	.984	.329	.496
	9	.000	.667	.500	.015	.656	.497 = (Cr_5)
	10	.333	.000	.750	.338	.002	.750
	11	.333	.333	.750	.345	.335	.750
	12	.333	.667	.750	.348	.668	.750
Si	1	.333	.333	.154	.336	.338	.152
	2	.333	.667	.154	.339	.672	.154
	3	.000	.000	.346	.004	.001	.348
	4	.000	.667	.346	.006	.671	.344
	5	.167	.167	.654	.170	.167	.656
	6	.167	.833	.654	.170	.837	.653
	7	.000	.000	.846	.992	.005	.844
	8	.000	.667	.846	.992	.671	.845
O	1	.110	.760	.134	.098	.760	.132
	2	.590	.730	.134	.590	.730	.138
	3	.310	.500	.134	.322	.512	.138
	4	.333	.333	.214	.333	.333	.214
	5	.333	.667	.214	.333	.667	.214
	6	.230	.567	.366	.215	.570	.371
	7	.730	.600	.366	.739	.620	.358
	8	.530	.333	.366	.514	.316	.369
	9	.000	.000	.286	.000	.000	.286
	10	.000	.667	.286	.000	.667	.286
	11	.410	.740	.634	.410	.732	.640
	12	.890	.760	.634	.914	.758	.634
	13	.690	.500	.634	.678	.508	.640
	14	.167	.167	.714	.167	.167	.714
	15	.167	.833	.714	.167	.833	.714
O	16	0.260	0.600	0.866	0.278	0.621	0.859
	17	.760	.567	.866	.778	.571	.872

[a] Coordinates are for polytype $\bar{x}_1$-Ia-5:x_3-IIa-4 with basal oxygen triad rotated 6°. Origin is in the brucite sheet.

TABLE 2 (*Continued*)

Atom	Ideal			Refined		
	x	*y*	*z*	*x*	*y*	*z*
18	0.460	0.333	0.866	0.450	0.328	0.867
19	.000	.000	.786	.000	.000	.786
20	.000	.667	.786	.000	.667	.786
OH 1	.333	.000	.967	.386	.002	.967
2	.333	.333	.967	.366	.347	.967
3	.333	.667	.967	.378	.667	.967
4	.167	.167	.034	.172	.155	.034
5	.167	.500	.034	.156	.504	.034
6	.167	.833	.034	.154	.826	.034
7	.333	.000	.214	.333	.000	.214
8	.000	.333	.286	.000	.333	.286
9	.167	.167	.467	.168	.167	.467
10	.167	.500	.467	.140	.505	.467
11	.167	.833	.467	.166	.843	.467
12	.333	.000	.534	.363	.002	.534
13	.333	.333	.534	.371	.327	.534
14	.333	.667	.534	.384	.648	.534
15	.167	.500	.714	.167	.500	.714
16	.000	.333	.786	.000	.333	.786

served reflections from 11 levels along the z axis were used. These reflections had been collected from the same elongate crystal before it was cut, using the Weissenberg multiple film pack technique and CuKα radiation. Absorption correction for a cylinder of the average diameter of the crystal was applied as an approximation. Also, Lorentz-polarization and $\alpha_1-\alpha_2$ separation corrections were applied. On the basis of these twin model intensity calculations the *Cc* structure twinned by 180° rotation around [010] was the only model that could not be proved invalid. This ideal structure has the *c*-glide perpendicular to the direction usually designated as the x axis (5.3 Å repeat) in layer silicates, and would require reversal of the customary x and y axes. The actual crystal, however, has only a pseudo *c*-glide, so that all indices and coordinates reported here are for the usual cell orientation.

A three-dimensional structure refinement was attempted for the *Cc* structure, using the space group *C*1 because of the observed pseudo symmetry. A least squares program was modified to twin the reciprocal lattice and to build up intensities in the same manner as the twinned crys-

tal. For 519 reflections[1] representing 0*kl*, *h*0*l*, *hk*0, and *hk*8 data the refinement progressed only to an *R* value of 19% from a starting value near 25%. The atomic parameters at this final stage are listed in Table 2. Several factors, including the problem of evaluating the exact volume of the two twin sets, the exact amount and distribution of the Cr ions in the brucite sheet, and the large number of variable parameters (165) in a 2-layer cell relative to the amount of data, are probably significant in preventing further progress of the refinement. In view of the high *R* factor the interatomic distances resulting from the refinement will not be reported. However, the major structural features, several of which can be deduced from the observed data and tests and are confirmed by the refinement, will be discussed briefly.

Discussion

One of the important features of the structure is the nature of the 2-layer packet that can be chosen on the basis of the *h*0*l* data. For the polytypes included in this projection group the generalized polytype designation is $\bar{x}$-I*a*-(1-3-5):*x*-II*a*-(2-4-6). In the first layer the talc octahedral sheet has site I occupied which requires that the upper part of the talc sheet be shifted along a $-x$ axis relative to the lower part of the sheet. The brucite sheet in the first layer is the I*a* type. In the second layer the alternate octahedral cation site in the talc sheet, site II, is occupied, which requires that the upper part of the talc sheet be shifted along a $+x$ axis. The brucite sheet of the second layer is a II*a* type. The alternate occupation of octahedral cation cites I, II, I, II . . . in the talc sheets and the alternate choice of I*a* and II*a* type brucite sheets are the major features contributing to the two-layer character of the structure.

The choice of alternate cation sites in the octahedral cation planes of the talc sheets of these crystals may also be the explanation for the twinning. If two different cation sites, I and II, are occupied in different regions or sectors of the same cation plane, the direction of stagger in the talc sheet will be different in those regions and a twinned structure will result.

The stability of this 2-layer structure can be compared best with 1-layer chlorite stabilities by considering each layer separately. If the second layer were rotated 60° to give it the same orientation as the first layer it would have the designation $\bar{x}_1$-I*a*-5, which is the enantiomorph

[1] The F_0 and F_c values for these reflections and for selected *hkl* reflections from the elongate crystal have been deposited as Document No. 9663 with the American Documentation Institute, Auxiliary Publications Project, Photoduplication Service, Library of Congress, Washington 25, D. C. Copies may be secured by citing the document number, and remitting in advance $1.25 for photoprints or for 35 mm microfilm.

of the first layer $\bar{x}_1$-Ia-3. All Ia-odd layer types, after 180° rotation about the y axis, are equivalent to, and should have the same relative stabilities as, the Ib ($\beta = 97°$) layer types described in Part I. As pointed out in Part III (Shirozu and Bailey, 1965), the talc sheet contacts are different on opposite sides of the brucite sheet in such layers. This asymmetric positioning of the talc sheets relative to the brucite sheets is maintained throughout the 2-layer packets studied here. Adoption in irregular sequence throughout the crystal of the three talc to brucite contacts that are possible for each layer would preserve the structural layer types and their asymmetric geometry, and would explain the streaking of $k \neq 3n$ reflections observed for the one crystal illustrated in Figure 5b. Even in this crystal there is a 2-layer periodicity that indicates the same layer types present and a regular alternation of occupation of the octahedral cation sites I and II in the talc and brucite sheets of adjacent layers.

The pseudo c-glide is a feature inherent in the structure. It is not caused by twinning because the $0kl$, $l \neq 2n$ reflections are also present on films of the untwinned segment. Rotation of the basal oxygen triads of the talc sheet, a feature common in layer silicates, does not destroy the c-glide that is present in the ideal model. More likely, the c-glide is destroyed by a special and uneven distribution of scattering power over cation sites related by a c-glide. Neither the tetrahedral cations nor the octahedral cations of the talc sheet can provide such an arrangement. Therefore the c-glide must be destroyed by a special distribution of Cr ions in the brucite sheet so that the Cr ions in alternating brucite sheets are not related by a c-glide. This is a feasible explanation because tests using $00l$ data to determine the distribution of octahedral cations between the talc and brucite sheets show that the Cr ion is entirely within the brucite sheet. This is also the case for the 1-layer polytype from this sample studied in Part II.

The concept of a special distribution of Cr ions in the brucite sheet was taken into consideration in testing the twinned models of the Cc and $Ccm2_1$ structures and in choosing the Cc structure as the correct trial model. In a 2-layer structure there are six different octahedral cation sites in the brucite sheets, three in the brucite sheet of the first layer and three in the brucite sheet of the second layer (Fig. 6a). The two Cr ions, one for each layer, that are available for distribution between these sites can be arranged in nine different Cr distribution patterns. The Cr distribution may preserve the c-glide or destroy it. The six Cr combinations that violate the c-glide are designated 1–5, 1–6, 2–4, 2–6, 3–4, and 3–5. From the tests of the twinned trial models it was possible to eliminate four of these combinations. A final choice between Cr distribution patterns 2–6 and 3–5 could not be made. For hkl, $l = 2n$, calculated data for

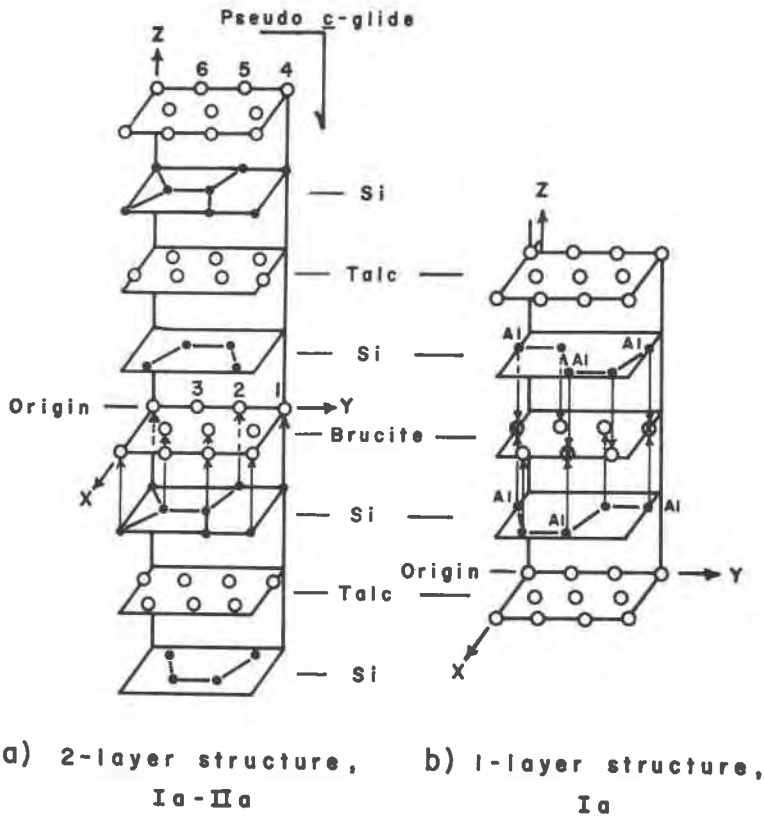

FIG. 6. Diagram of planes of cations. The arrow connects superimposing cations. (a) 2-layer structure, I*a*-II*a*. (b) 1-layer structure, I*a*-4 (Brown and Bailey, 1963). Chromium position in the brucite sheet is marked with an *x*.

the 2–6 and 3–5 patterns are exactly the same, and for hkl, $l \neq 2n$, the calculated data are the same after twinning.

The restriction of Cr to sites 2 and 6 (or 3 and 5) may give a clue to possible Al ordering in the tetrahedral sheet. Brown and Bailey (1963) found local charge balance in the structure of a 1-layer Cr chlorite, I*a*-4, such that the Cr^{3+} ion was located directly between the tetrahedral sites in the talc sheets above and below that contained the most substitution of Al^{3+} for Si^{4+} (Fig. 6*b*). By analogy with this structure Al may be inferred to substitute for Si in the tetrahedral site of the talc sheet directly below the Cr-rich brucite cation site 2 (or 5). Brucite cation site 6 (or 3) is a site of no cation repulsion and would also be a favorable site for Cr ions.

Although twinning prevented complete refinement, it was still possible

to determine the direction and approximate amount of rotation of the tetrahedra. As in other layer silicate structures, the basal oxygen triad of the talc sheet has rotated from its ideal position in the direction to obtain optimum hydrogen bonds between the tetrahedral basal oxygens and the brucite hydroxyls. The amount of rotation is approximately 6°, which is the same as that reported by Brown and Bailey (1963) for a 1-layer Cr chlorite from the same locality. The presence of very weak $06l, l \neq 2n$ reflections also suggest that some atoms that ideally repeat at intervals of $b/3$ must be displaced from this ideal relationship. These displacements could not be determined.

Acknowledgments

This study was supported in part by grant 1176-A2 from the Petroleum Research Fund, administered by the American Chemical Society, in part by National Science Foundation grant GP-4843, and in part by the Research Committee of the Graduate School from funds supplied by the Wisconsin Alumni Research Foundation. Computations were carried out in the University of Wisconsin Computing Center, which is also supported in part by National Science Foundation funds.

References

Bailey, S. W. and B. E. Brown (1962) Chlorite polytypism: I. Regular and semi-random one-layer structures. *Amer. Mineral.* **47,** 819–850.

Brindley, G. W. (1961) Chlorite minerals. In Brown, G., ed., *The X-ray Identification and Crystal Structures of Clay Minerals* (2nd ed.), chap. 6. Mineral. Soc., London.

———, Beryl Oughton, and K. Robinson (1950) Polymorphism of the chlorites. I. Ordered structures. *Acta Crystallogr.* **3,** 408–416.

Brown, B. E. and S. W. Bailey (1963) Chlorite polytypism: II. Crystal structure of a one-layer Cr-chlorite. *Amer. Mineral.* **48,** 42–61.

Drits, V. A. (1966) X-ray investigation of some rare polytypes of layer silicates. *Acta Crystallogr.* 21, A172.

Frondel, C. (1955) Two chlorites: gonyerite and melanolite. *Amer. Mineral.* **40,** 1090–1094.

Lister, Judith S. (1966) *The crystal structure of two chlorites.* Ph.D. Thesis, Univ. Wisconsin.

Mathieson, A. McL. and G. F. Walker (1954) Crystal structure of magnesium-vermiculite. *Amer. Mineral.* **39,** 231–255.

Sadanaga, R. and Y. Takéuchi (1961) Polysynthetic twinning of micas. *Z. Kristallogr.* **116,** 406–429.

Shirozu, Haruo and S. W. Bailey (1965) Chlorite polytypism: III. Crystal structure of an orthohexagonal iron chlorite. *Amer. Mineral.* **50,** 868–885.

——— (1966) Crystal structure of a two-layer Mg-vermiculite. *Amer. Mineral.* **51,** 1124–1143.

Weisz, O., W. Cochran and W. F. Cole (1948) The accurate determination of cell dimensions from single-crystal X-ray photographs. *Acta Crystallogr.* **1,** 83–88.

Manuscript received April 14, 1967; accepted for publication June 30, 1967.